# SUPPORTING INFORMATION

## MATERIALS AND METHODS

**Immunofluorescence.** Aortas and brains were excised, frozen in O.C.T. compound (Sakura), sectioned in 7-μm slices, and fixed with 4% paraformaldehyde prior to staining with Alexa-Fluor conjugated secondary antibodies (Invitrogen). Specific proteins were identified with primary antibodies: FITC conjugated rabbit anti β-galactosidase (Immunology Consultant Laboratory), goat anti-mouse Notch 3 (R&D Systems), Cy3 conjugated mouse anti-α-smooth muscle actin clone 1A4 (Sigma), goat anti-mouse Notch 3 (M-20, Santa Cruz Biotechnology). Samples were examined on a Nikon Eclipse 80i Upright Microscope and images captured with a digital camera (Hamamatsu Orca 100) using imaging software MetaMorph 7.

**Electron Microscopy.** Brain tissue was fixed by transcardiac perfusion with 2.5% glutaraldehyde, 2% paraformaldehyde in 0.1M sodium cacodylate buffer (pH 7.4), rinsed, dehydrated in a series of ethanol dilutions (50–100%), and embedded in epoxy resin (EMbed 812; Electron Microscopy Sciences). Ultrathin sections (60 nm) were cut on a Reichert ultramicrotome and collected on Formvar- and carbon-coated grids. The samples were stained with 2% uranyl acetate and lead citrate and examined on a Philips Tecnai 12 BioTWIN electron microscope (FEI Co.). Images were captured digitally using a CCD camera (Morada; Soft Imaging Systems).

**FACS.** Sorting was performed on a 3-laser FACSAria high-speed cell sorter (BD Biosciences), with a 70 μm nozzle and at a sheath pressure of 70 psi. Sample

temperature was maintained at 4°C during sorting. Selection was based on a broad FSC/SSC gate to eliminate debris and large aggregates, and the brightest 0.5% fluorescein-positive events were sorted, as measured in 530/30 and 575/26 bandpass filters.

**RNA extraction and quality control.** For RNA preparation, brain-derived cells were sorted directly into extraction buffer (RNAeasy, Qiagen) supplemented with 3% ß-mercaptoethanol and purified according to the manufacturer's instructions. Samples were treated with DNAse prior to analysis (Invitrogen). All samples were controlled for RNA quality by microcapillary electrophoresis (RNA 6000 Pico Assay, Agilent Technologies, Palo Alto, CA). Only the samples showing RNA integrity as judged by the presence of sharp 18S and 28S ribosomal RNA peaks, and displaying no obvious signs of RNA degradation in the fluorograms were considered for subsequent microarray hybridization.

**RNA amplification.** RNA samples from freshly sorted brain SMC extracts were amplified using the RiboAMP HS amplification system (Molecular Devices/MDS – Sunnyvale, CA) for 1.5 rounds of amplification. This was followed by an *in vitro* transcription round using the Enzo BioArray T7 RNA transcript labeling system (Enzo Life Sciences, Farmingdale, NY) to biotinylate the RNA. Biotinylated RNAs were purified via Qiagen RNeasy Mini column RNA cleanup protocol, and eluted in two steps using first 25 µl and then 15 µl of RNAse-free water. The purified biotin-containing transcripts were then analyzed via Agilent RNA 6000 Nano chip to determine complexity and transcript length. Only IVT samples with comparable complexity and transcript lengths were hybridized to the Affymetrix arrays.

**Measurement of Absolute Cerebral Blood Flow.** Absolute CBF (aCBF) was measured using an indicator fractionation technique (12). Briefly, the left femoral artery and right jugular vein of anesthetized mice were cannulated. The mice received 1 μCi of N-isopropyl-[methyl 1,3-$^{14}$C]-*p*-iodoamphetamine from the right jugular vein as a bolus. One hundred μL of arterial blood samples from the femoral artery were collected for 20 seconds (0.3 mL/min). Then the mice were decapitated and the whole brain was removed and immediately frozen in chilled isopentane solution. The frozen brains dissected into left and right hemispheres were weighted and digested with Scintigest solution (Fischer Scientific) at 50 for 6h. Scintillation fluid and $H_2O_2$ were added to the sample and twelve hours after shaking, radioactivity in the blood and brain samples was measured by liquid scintillation spectrometry (RackBeta 1209; Pharmacia Wallac). aCBF was calculated as follows: CBF (ml/100 g/min) = (brain count (cpm)x0.3(ml/min)/(blood count (cpm)xbrain weight (g))x100.

**Functional studies of contractile activity in isolated aorta.** Mice were sacrificed by decapitation. Aorta was removed and immersed in physiological solution (composition, mM: NaCl, 118; KCl, 4.6; $NaHCO_3$, 25; $MgSO_4$, 1.2; $KH_2PO_4$, 1.2; $CaCl_2$, 1.25; glucose, 10; EDTA, 0.025; pH 7.4 at 37°C). After removing the surrounding connective tissue, aorta was cut into segments (2 mm long), threaded onto 40 μm stainless steel wires and mounted in a isometric myograph (610M, Danish Myo Technology, Aarhus, Denmark). After mounting, each preparation was equilibrated, unstretched, for 30 min in physiological solution, maintained at 37°C and aerated with a gas mixture of 95% $O_2$ - 5% $CO_2$. Then, the normalized passive resting force and the corresponding diameter were determined for each preparation from its own length-pressure curve, according to

Mulvany and Halpern (1977). Contractile responses were recorded into a computer, by using a data acquisition and recording software (Myodaq and Myodata, Danish Myo Technology). After normalization and a 30-min equilibration in physiological solution, the preparations were stimulated with isotonic depolarizing 100 mM KCl solution, in which part of NaCl had been replaced by equimolar amount of KCl. After washout, the preparations were challenged with cumulative concentrations of phenylephrine (PE, 1 nM - 1 μM); on the top of PE-induced contraction cumulative concentrations of acetylcholine (ACh, 1 nM - 1 μM) were added, to assess endothelium/nitric oxide-dependent vasodilatation. PE, ACh, L-NAME and SNP were from Sigma (S. Louis, MO); 10 mM stock solution were prepared in $H_2O$ and further dissolved in physiological solution as required.

**Measurement of Physiological Variables.** Regional CBF (rCBF), Mean arterial blood pressure (MABP), arterial blood gases ($pO_2$, $pCO_2$, pH), and rectal temperature were measured as described previously (11, 26). Briefly, rCBF was measured by laser Doppler flowmetry (Perimed) with a flexible 0.8-mm fiberoptic extension. The tip of probe was affixed to the intact skull over the left cortex (2 mm posterior and 6 mm lateral from bregma). MABP was obtained from the left femoral artery. Arterial blood gases ($pO_2$ and $pCO_2$) and pH were measured 10 min before ischemia and 30 min after reperfusion. Rectal temperature was maintained at 37°C.

**FIGURE LEGENDS**

**SI Fig. 6.** *Notch 3* expression. In situ hybridization with a *Notch 3* antisense riboprobe reveals strong expression in the ventricular zone at E13.5 (A, B; sections at two different levels of the same embryo), which persists at E15.5; note low levels of expression in the developing thalamus (C). At early postnatal stages, in addition to the vasculature, *Notch 3* mRNA is also detected in thalamic nuclei (D). cc: corpus callosum; hip: hippocampus; thal: thalamus.

**SI Fig. 7.** Electron microscopy analysis. Electron micrographs of arterial cortical vessels (top four panels) and tunica media of aorta (bottom four panels) from 8-week-old wild type (left) and *Notch 3* –/– (right) mice. No differences were observed in the structure of the vessels or the morphology of cytoplasmic organelles in smooth muscle cells. sm: smooth muscle cells; e: endothelial cells of the tunica intima; L: lumen. Scale bar: 1μm.

**SI Fig. 8.** Characterization of brain-derived FACS sorted cells. Plasma membrane localization of Notch 3 was detected in BrSMC derived from *Notch 3* +/– but not from *Notch 3* –/– mice using antibodies raised against the extracellular domain of the protein (extra). In Notch 3 –/– cells, expression of the fusion protein was restricted to perinuclear structures as expected for the trapped protein created by the insertional mutagenesis. As predicted, antibody staining did not detect expression of the intracellular domain of Notch 3 (intra) in cells derived from *Notch 3* –/– animals but stained both the plasma membrane and cytoplasmic structures in cells from *Notch 3* +/– mice.

**SI Fig. 9.** Carbon-black analysis of brain vessels. The anatomy of the circle of Willis was studied using intracardiac carbon black ink perfusion in wild-type (WT; n=5) and *Notch 3* –/– mice (N3–/–; n=3). Ventral views of representative carbon black-perfused brains are labeled with red circles. Identified major arteries of circle of Willis are labeled with red dotted circles. No phenotypic difference was observed in circle of Willis anatomy between the mouse strains. Posterior communicating arteries, a common route for collateral blood flow in focal ischemia models, were present in all mice studied. ACA, anterior cerebral artery; MCA, middle cerebral artery; ICA, internal carotid artery; PCA, posterior cerebral artery; PComm, posterior communicating artery; BA, basilar artery.

**SI Fig. 10.** Functional studies of contractile and relaxation activity in isolated aorta. Physiological responses of isolated aortic segments were assessed in an isometric myograph. (A) Contractile responses to 100 mM KCl-induced depolarization (calcium influx through voltage-dependant calcium channels). (B) Contractile responses to cumulative concentrations of phenylephrine (PE, alpha-adrenergic receptor-stimulation). (C) Endothelium-dependent vasodilatation to cumulative concentrations of acetylcholine (ACh, known to promote eNOS activation in endothelial cells through muscarinic receptors). ACh was added on the plateau of the contraction to 1 μM PE. Mean from 2-4 preparations per mouse; standard deviation bars in (B) and (C) are omitted for clarity; they did not exceed 10% of the mean. WT, n=5; *Notch 3* –/–, n=9; *Notch 3* +/–, n=8. Neither the vasocontraction to KCl or PE, nor the vasodilation to ACh or sodium

nitroprusside (data not shown) were significantly different in the three groups. All animals were 10-12 week-old male mice.

SI Figure 6.

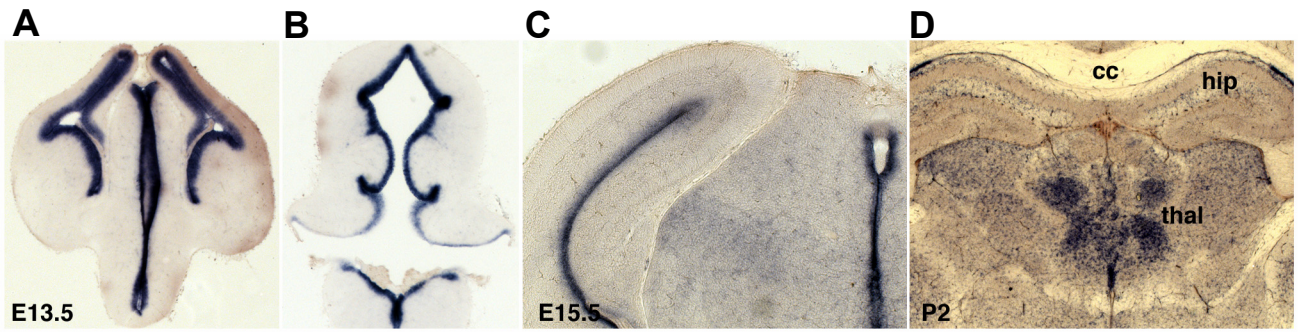

SI Figure 7.

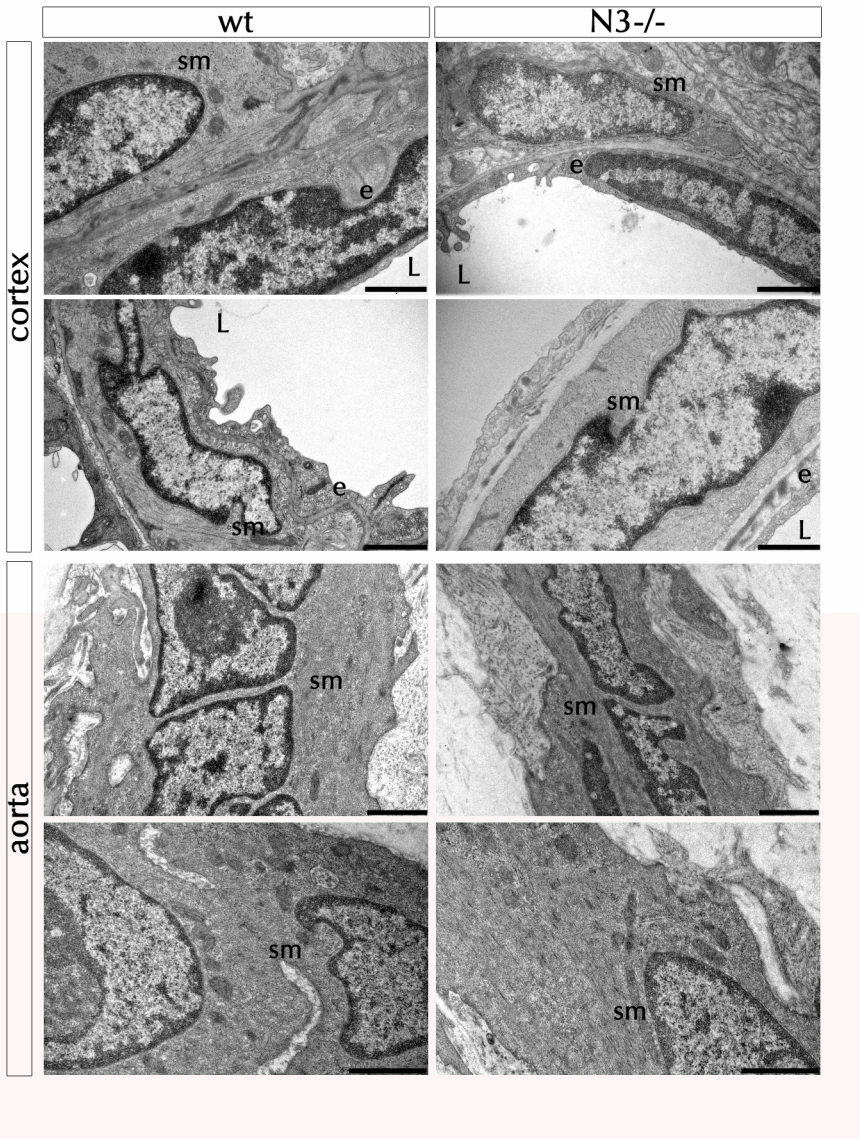

SI Figure 8.

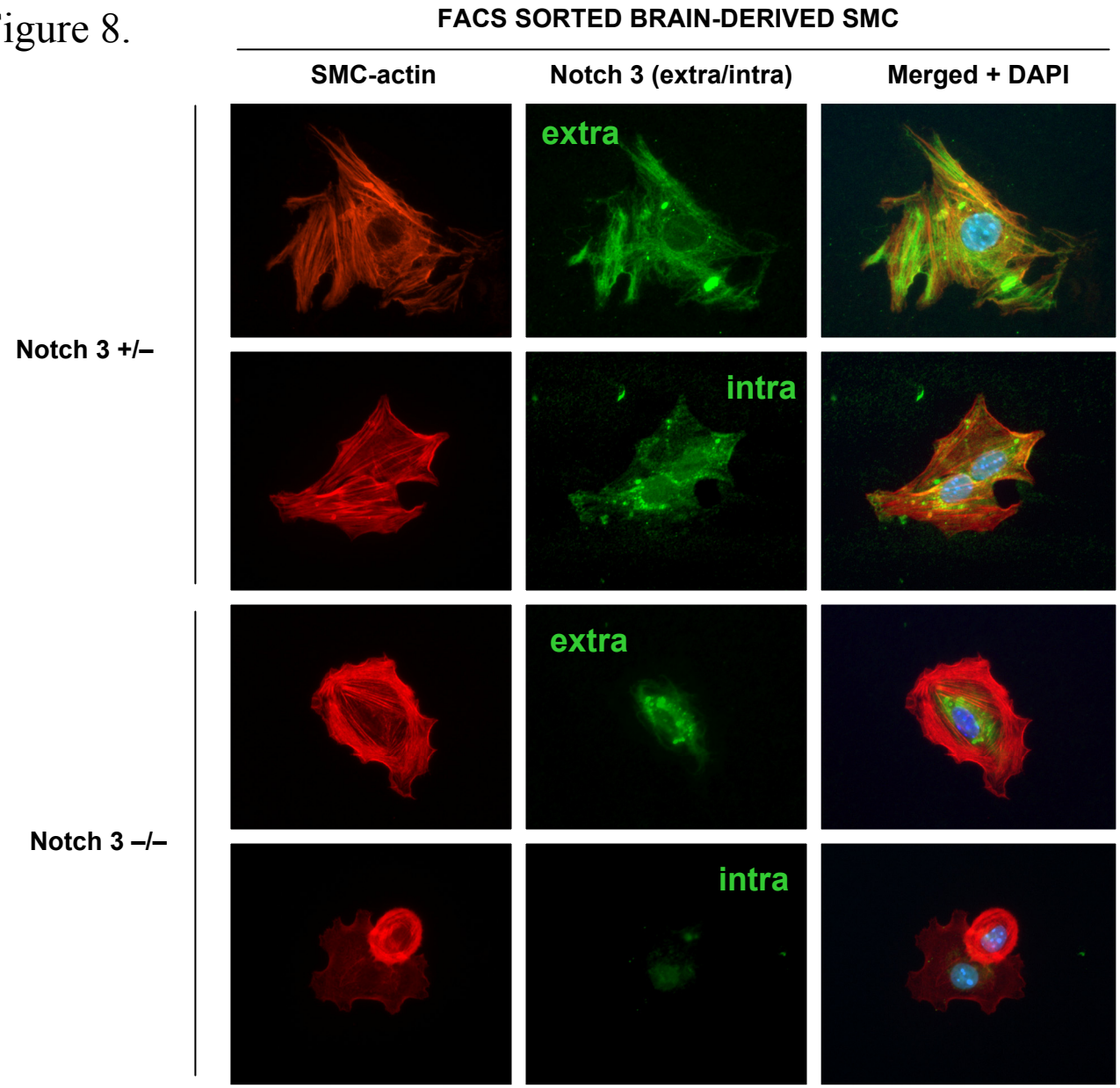
FACS SORTED BRAIN-DERIVED SMC
SMC-actin
Notch 3 (extra/intra)
Merged + DAPI
extra
intra
extra
intra
Notch 3 +/–
Notch 3 –/–

SI Figure 9.

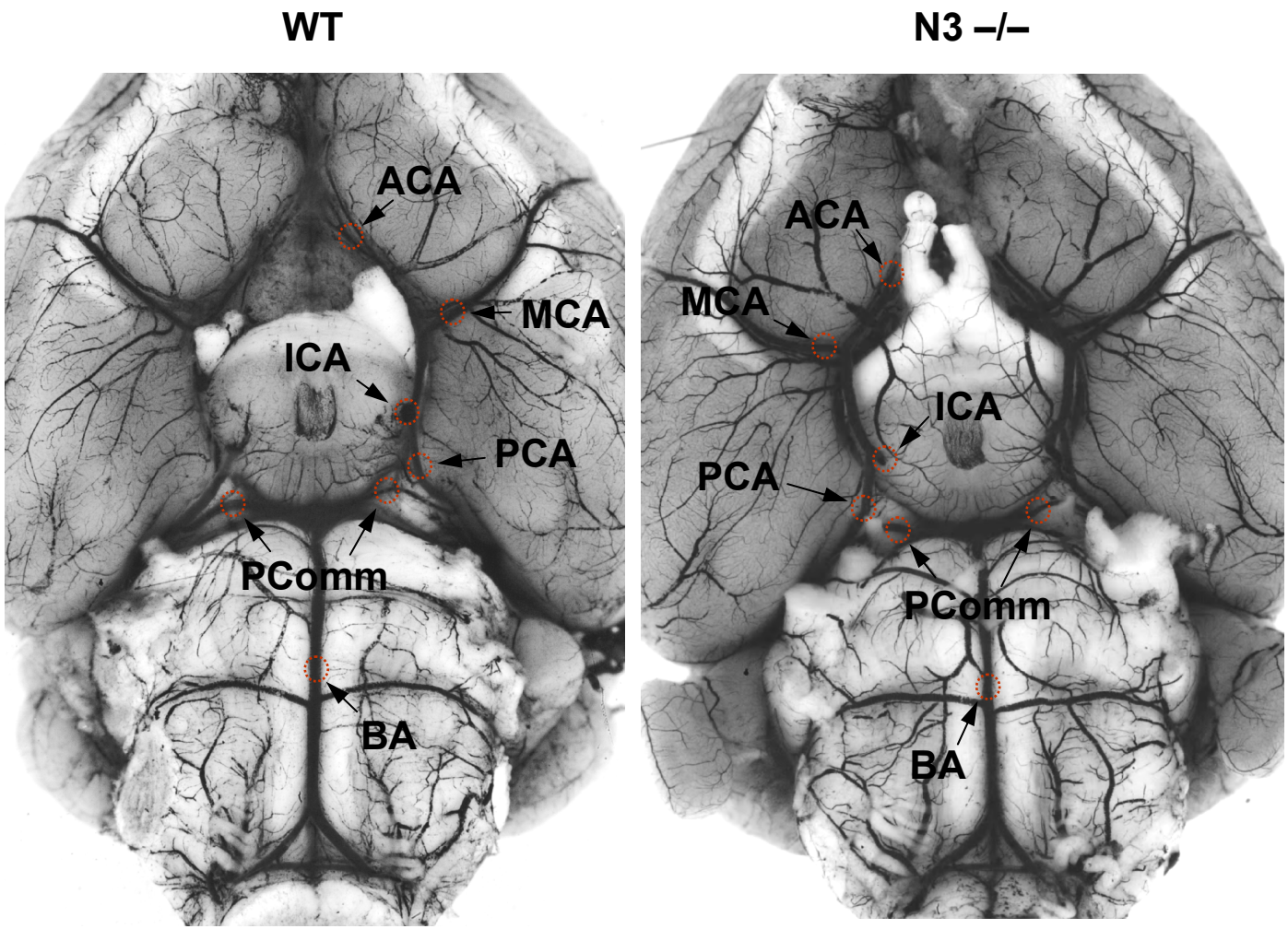

SI Figure 10.

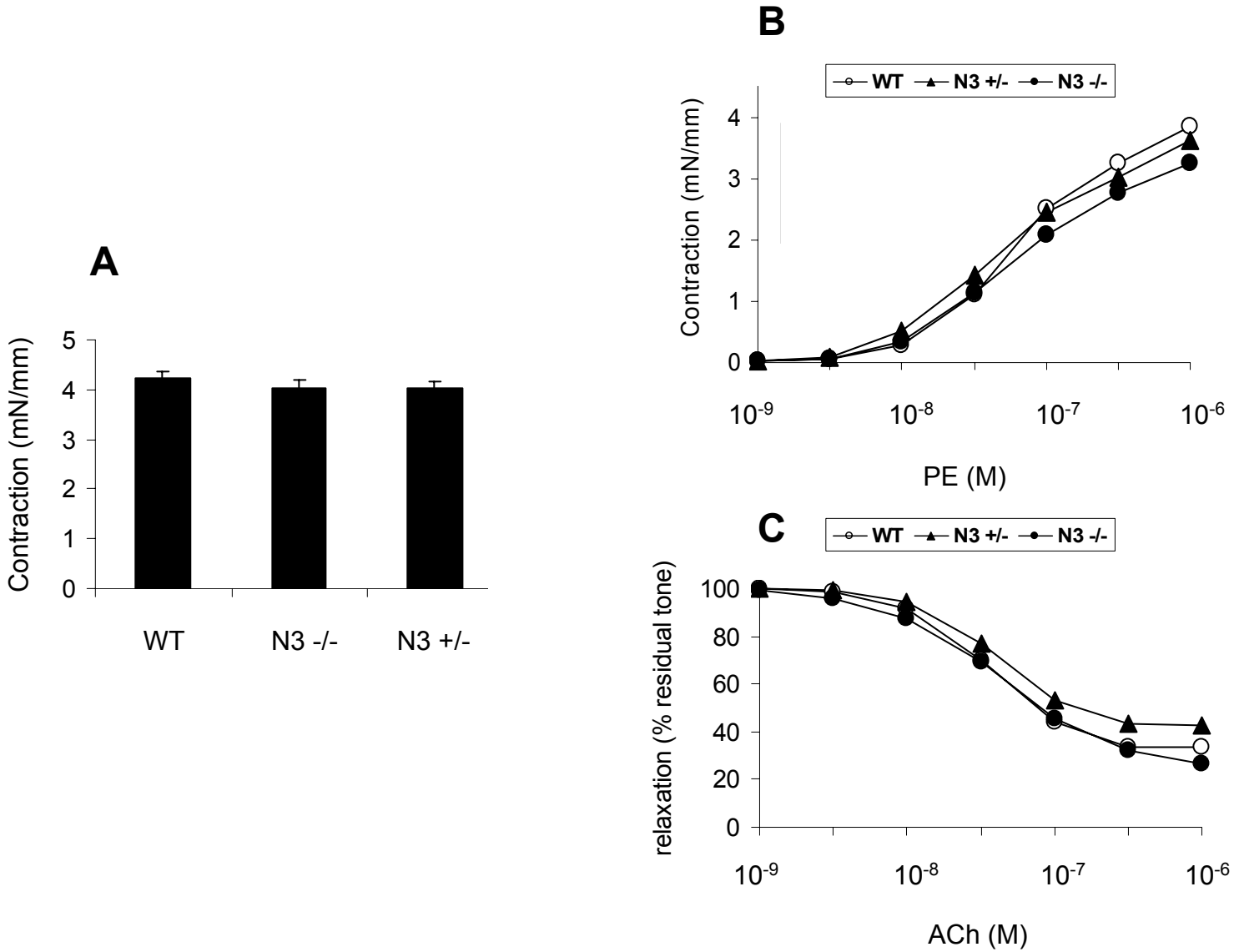
A
Contraction (mN/mm)
0
1
2
3
4
5
WT
N3 -/-
N3 +/-
B
WT
N3 +/-
N3 -/-
Contraction (mN/mm)
0
1
2
3
4
10-9
10-8
10-7
10-6
PE (M)
C
WT
N3 +/-
N3 -/-
relaxation (% residual tone)
0
20
40
60
80
100
10-9
10-8
10-7
10-6
ACh (M)

**SI Table 1. Gene ontology analysis of misregulated genes in brain-derived SMC from *Notch 3* –/– mice.**

| BIOLOGICAL PROCESS | Ref. IDs. | Reg. IDs. | Expected | +/- | p value |
|---|---|---|---|---|---|
| Muscle contraction | 111 | 16 | 2.26 | + | 6.14E-08 |
| Cell structure and motility | 759 | 30 | 15.48 | + | 1.43E-02 |
| Muscle development | 89 | 9 | 1.82 | + | 2.13E-02 |
| Mesoderm development | 365 | 19 | 7.45 | + | 3.18E-02 |

Gene set enrichment analyses revealed categories of genes misregulated in BrSMC from *Notch 3* –/– mice. -Ref. IDs- corresponds to gene accession numbers represented in the microarray belonging to a specific category while -Reg. IDs- stands for gene accession numbers found to be misregulated in the sample. -Expected- refers to gene accession numbers stochastically expected to appear in the list of regulated genes, based on the reference list. (+/–) indicates whether gene accession numbers from a given category are over (+) or under-represented (–).

**SI Table 2 *A-D*. Functional categories of genes misregulated in BrSMC from *Notch 3* –/– mice.**

## *A*. Muscle contraction

| Sequence Code | Primary Name | Accession # | Sequence Description | Fold Change | P-value |
|---|---|---|---|---|---|
| 1418604_at | Avpr1a | D49729 | Arginine vasopressin receptor 1A | -1.67019 | 4.72E-03 |
| 1423365_at | Cacna1g | AW494038 | Calcium channel, voltage-dependent, T type, alpha 1G subunit | -3.30521 | 2.72E-16 |
| 1451955_a_at | Cacna2d2 | AF247140 | Voltage-dependent calcium channel alpha-2-delta-2 mutant subunit 1 | -5.32064 | 6.90E-04 |
| 1460513_a_at | Ednra | AK017486 | ENDOTHELIN-1 RECEPTOR PRECURSOR (ET-A) | -2.55463 | 4.05E-03 |
| 1421400_at | Kcnmb1 | BB633976 | Potassium large conductance calcium-activated channel, subfamily M, beta member 1 | -1.64268 | 8.76E-03 |
| 1424269_a_at | Myl6 | BC026760 | Myosin, light polypeptide 6, alkali, smooth muscle and non-muscle | -1.89359 | 9.05E-12 |
| 1452670_at | Myl9 | AK007972 | Myosin regulatory light polypeptide 9 | -2.87804 | 2.63E-08 |
| 1425506_at | Mylk | BF451748 | Myosin, light polypeptide kinase | -1.64055 | 4.20E-04 |
| 1427228_at | Palld | AF205078 | MKIAA0992 protein | -2.26717 | 2.80E-04 |
| 1433768_at | Palld | BG071905 | MKIAA0992 protein | -1.65443 | 5.00E-05 |
| 1423505_at | Tagln | BB114067 | Transgelin | -2.3503 | 2.40E-12 |
| 1426529_a_at | Tagln2 | C76322 | Transgelin 2 | -1.60007 | 2.00E-05 |
| 1423049_a_at | Tpm1 | AK002271 | Tropomyosin 1, alpha | -2.99485 | 6.00E-04 |
| 1423721_at | Tpm1 | M22479 | Tropomyosin 1, alpha | -1.82762 | 1.77E-12 |
| 1449577_x_at | Tpm2 | AK003186 | Tropomyosin 2, beta | -1.91455 | 5.02E-06 |
| 1425028_a_at | Tpm2 | BC024358 | Tropomyosin 2, beta | -1.86385 | 7.52E-06 |

***B*. Cell structure and motility**

| Sequence Code | Primary Name | Accession # | Sequence Description | Fold Change | P-value |
|---|---|---|---|---|---|
| 1423222_at | Cap2 | AV261931 | CAP, adenylate cyclase-associated protein, 2 | -1.65898 | 1.60E-03 |
| 1421007_at | Col4a6 | BB794645 | Procollagen, type IV, alpha 6 | -1.65223 | 5.89E-03 |
| 1450625_at | Col5a2 | AV229424 | Procollagen, type V, alpha 2 | 1.79223 | 1.48E-03 |
| 1453099_at | Csnk2a2 | BG070990 | Casein kinase II, alpha 2, polypeptide | 1.51591 | 1.03E-03 |
| 1426731_at | Des | AI156158 | Desmin | -2.13638 | 2.15E-03 |
| 1428257_s_at | Dynlrb1 | BG791323 | Dynein, cytoplasmic, light chain 2A | -1.7935 | 5.91E-03 |
| 1426677_at | Flna | BM233746 | Filamin, alpha | -1.90315 | 2.85E-15 |
| 1460028_at | Grip2 | AI426339 | Glutamate receptor interacting protein 2 | -2.11795 | 8.60E-04 |
| 1454243_at | Ick | AK008991 | Intestinal cell kinase | 1.50375 | 5.44E-03 |
| 1427485_at | Lmod1 | AF237627 | Leiomodin 1 (smooth muscle) | -1.96143 | 3.51E-03 |
| 1425263_a_at | Mbp | BB181247 | Myelin basic protein, transcript variant 2 | 1.56877 | 9.19E-03 |
| 1448962_at | Myh11 | BC026142 | Myosin, heavy polypeptide 11, smooth muscle | -2.6623 | 7.57E-11 |
| 1452670_at | Myl9 | AK007972 | PREDICTED: myosin regulatory light polypeptide 9 | -2.87804 | 2.63E-08 |
| 1425506_at | Mylk | BF451748 | Myosin, light polypeptide kinase | -1.64055 | 4.20E-04 |
| 1427228_at | Palld | AF205078 | MKIAA0992 protein | -2.26717 | 2.80E-04 |
| 1433768_at | Palld | BG071905 | MKIAA0992 protein | -1.65443 | 5.00E-05 |
| 1449187_at | Pdgfa | BB371842 | Platelet derived growth factor, alpha | -1.60717 | 2.40E-04 |
| 1428319_at | Pdlim7 | AK010339 | PDZ and LIM domain 7 | -1.83779 | 9.80E-04 |
| 1449028_at | Rhou | AF378088 | Ras homolog gene family, member U | 2.55683 | 1.18E-03 |
| 1455197_at | Rnd1 | BE852181 | Rho family GTPase 1 | -2.2797 | 5.90E-04 |
| 1431732_at | Spag16 | AK015884 | Sperm associated antigen 16 (Spag16), transcript variant 1 | 3.23843 | 1.98E-03 |
| 1441507_at | Spnb2 | AW550681 | L0067G05-3 | 2.33802 | 2.93E-06 |
| 1424272_at | Stat3 | BC003806 | Signal transducer and activator of transcription 3 | -1.99279 | 6.64E-03 |
| 1455183_at | Stk38l | AV257215 | Serine/threonine kinase 38 like | -1.71224 | 1.32E-06 |
| 1419097_a_at | Stom | AF093620 | Stomatin | -2.59533 | 9.00E-05 |
| 1423049_a_at | Tpm1 | AK002271 | Tropomyosin 1, alpha | -2.99485 | 6.00E-04 |
| 1423721_at | Tpm1 | M22479 | Tropomyosin 1, alpha | -1.82762 | 1.77E-12 |
| 1449577_x_at | Tpm2 | AK003186 | Tropomyosin 2, beta | -1.91455 | 5.02E-06 |
| 1425028_a_at | Tpm2 | BC024358 | Tropomyosin 2, beta | -1.86385 | 7.52E-06 |
| 1428026_at | Tshz2 | BC028776 | Serologically defined colon cancer antigen 33 like | 1.81681 | 1.78E-03 |

## *C*. Muscle development

| Sequence Code | Primary Name | Accession # | Sequence Description | Fold Change | P-value |
|---|---|---|---|---|---|
| 1431339_a_at | Efhd2 | AK007560 | EF hand domain containing 2 (Efhd2) | -1.82704 | 7.78E-03 |
| 1427485_at | Lmod1 | AF237627 | Leiomodin 1 (smooth muscle) (Lmod1) | -1.96143 | 3.51E-03 |
| 1448962_at | Myh11 | BC026142 | Myosin, heavy polypeptide 11, smooth muscle | -2.6623 | 7.57E-11 |
| 1452670_at | Myl9 | AK007972 | PREDICTED: myosin regulatory light polypeptide 9 | -2.87804 | 2.63E-08 |
| 1425828_at | Nkx6-1 | AF357883 | NK6 transcription factor related, locus 1 (Drosophila) (Nkx6-1) | -2.39776 | 1.70E-04 |
| 1423721_at | Tpm1 | M22479 | Tropomyosin 1, alpha | -1.82762 | 1.77E-12 |
| 1423049_a_at | Tpm1 | AK002271 | Tropomyosin 1, alpha | -2.99485 | 6.00E-04 |
| 1449577_x_at | Tpm2 | AK003186 | Tropomyosin 2, beta | -1.91455 | 5.02E-06 |
| 1425028_a_at | Tpm2 | BC024358 | Tropomyosin 2, beta | -1.86385 | 7.52E-06 |

***D*. Mesoderm development**

| Sequence Code | Primary Name | Accession # | Sequence Description | Fold Change | P-value |
|---|---|---|---|---|---|
| 1418604_at | Avpr1a | D49729 | Arginine vasopressin receptor 1A | -1.67019 | 4.72E-03 |
| 1427183_at | Efemp1 | BC023060 | Epidermal growth factor-containing fibulin-like extracellular matrix protein 1 (Efemp1) | 1.83816 | 8.00E-04 |
| 1431339_a_at | Efhd2 | AK007560 | EF hand domain containing 2 | -1.82704 | 7.78E-03 |
| 1427485_at | Lmod1 | AF237627 | Leiomodin 1 (smooth muscle) | -1.96143 | 3.51E-03 |
| 1434900_at | Mkl1 | BM196656 | MKL (megakaryoblastic leukemia)/myocardin-like 1 | -2.60843 | 1.54E-03 |
| 1417127_at | Msx1 | BC016426 | Homeo box, msh-like 1 | -1.55581 | 1.50E-03 |
| 1448962_at | Myh11 | BC026142 | Myosin, heavy polypeptide 11, smooth muscle | -2.6623 | 7.57E-11 |
| 1452670_at | Myl9 | AK007972 | Myosin regulatory light polypeptide 9 | -2.87804 | 2.63E-08 |
| 1425828_at | Nkx6-1 | AF357883 | NK6 transcription factor related, locus 1 | -2.39776 | 1.70E-04 |
| 1426981_at | Pcsk6 | BI157485 | Proprotein convertase subtilisin/kexin type 6 | -1.77147 | 8.00E-03 |
| 1428319_at | Pdlim7 | AK010339 | PDZ and LIM domain 7 | -1.83779 | 9.80E-04 |
| 1417654_at | Sdc4 | BC005679 | Syndecan 4 | -1.57365 | 1.49E-03 |
| 1429459_at | Sema3d | BB499147 | Sema domain, immunoglobulin domain (Ig), short basic domain, secreted, (semaphorin) 3D | 3.15043 | 9.00E-05 |
| 1436240_at | Sost | BM211445 | RIKEN cDNA 1500010G04 | 23.81789 | 4.69E-09 |
| 1424272_at | Stat3 | BC003806 | Signal transducer and activator of transcription 3 | -1.99279 | 6.64E-03 |
| 1423049_a_at | Tpm1 | AK002271 | Tropomyosin 1, alpha | -2.99485 | 6.00E-04 |
| 1423721_at | Tpm1 | M22479 | Tropomyosin 1, alpha | -1.82762 | 1.77E-12 |
| 1449577_x_at | Tpm2 | AK003186 | Tropomyosin 2, beta | -1.91455 | 5.02E-06 |
| 1425028_a_at | Tpm2 | BC024358 | Tropomyosin 2, beta | -1.86385 | 7.52E-06 |

The list of gene accession numbers from each category indicates the Affymetrix number (sequence code) and also the fold change using the signal found in Notch 3 +/– samples as baseline. Some unique genes were represented in both the reference list and the list of regulated sequences by several accession numbers with their corresponding fold change and p-value.

**SI Table 3. Physiological variables.**

| Genotype | Condition | R.T. (oC ) | pH | PaCO2 (mmHg) | PaO2 (mmHg) | MABP (mmHg) |
|---|---|---|---|---|---|---|
| | Pre | 36.7±0.2 | 7.39±0.02 | 37.4±4.8 | 176±11 | 103±14 |
| | MCAo | 36.4±0.2 | 7.37±0.02 | 38.8±5.9 | 180±5 | 97±12 |
| WT | Post | 36.1±0.3 | 7.29±0.03 | 39.4±5.8 | 188±12 | 100±10 |
| | Pre | 36.7±0.3 | 7.39±0.03 | 35.9±3.8 | 174±7 | 105±7 |
| | MCAo | 36.5±0.5 | 7.42±0.05 | 41.2±5.0 | 180±14 | 102±9 |
| Notch 3 +/- | Post | 36.2±0.3 | 7.29±0.02 | 48.2±2.5 | 184±12 | 102±9 |
| | Pre | 36.6±0.2 | 7.39±0.02 | 36.3±4.0 | 170±21 | 94±7 |
| | MCAo | 36.6±0.4 | 7.37±0.05 | 39.9±5.1 | 182±19 | 94±8 |
| Notch 3 -/- | Post | 36.2±0.4 | 7.32±0.04 | 38.6±3.6 | 191±23 | 95±8 |

Values are given as mean ± s.d. R.T., rectal temperature; MABP, mean arterial blood pressure.